Mössbauer and atom probe studies on the ferrite decomposition in duplex stainless steels caused by the quenching rate

1999 J. Phys.: Condens. Matter 11 1105

(http://iopscience.iop.org/0953-8984/11/4/018)

J. Phys.: Condens. Matter **11** (1999) 1105–1114. Printed in the UK PII: S0953-8984(99)97615-4

Mössbauer and atom probe studies on the ferrite decomposition in duplex stainless steels caused by the quenching rate

C Lemoine, A Fnidiki, F Danoix, M Hédin and J Teillet

Groupe de Métallurgie Physique UMR CNRS 6634, 76821 Mont-Saint-Aignan Cédex, France

Received 16 September 1998

Abstract. The structural and magnetic properties of duplex stainless steels have been studied by conversion electron Mössbauer spectrometry (CEMS) and atom probe. The results prove that the quenching rate Q is responsible for ferrite embrittlement of duplex stainless steels. This embrittlement, due to ferrite decomposition, increases when Q decreases. The Mössbauer spectrometry has been proved to be appropriate to study the early stages of the transformation. From the hyperfine field distribution of the very decomposed ferrite, the concentration of the α Fe-enriched domains and the α' Cr-enriched domains have been estimated and compared with results obtained by atom probe.

1. Introduction

Duplex stainless steels are quite appropriate when stainless properties are required in parallel with good tensile strength. The great limitation of such steels is their embrittlement during thermal ageing below 475 °C. This results in a loss of mechanical properties due to ferrite decomposition, via a spinodal process, into an interconnected network of homophase α Fe-enriched and α' Cr-enriched domains [1–3]. Thermal ageing effects in ferrite have been widely studied in the last twenty years, as well as in Fe–Cr alloys [4–6], in simple ferritic alloys [7, 8], and in duplex steels [4, 8]. Some previous works have reported that ferrite may already be decomposed even before thermal ageing. Sassen *et al*, working on the kinetics of ferrite transformation in duplex stainless steels, concluded that a decomposition can be detected in solution-treated material even after water quenching [3]. Likewise, Pollak *et al*, studying ferritic stainless steel embrittlement at 475 °C, has reported that segregation already exists before ageing [9]. More recently, atom probe analyses have shown that concentration amplitude fluctuations already exist in unaged duplex steels, and have proved that the rate of development of these fluctuations increases with decreasing quenching rate [10]. These results were confirmed, using Mössbauer spectrometry results on several unaged specimens [11]. Nevertheless, the mechanism of ferrite transformation during the quench is not well known.

The ferrite decomposition during the quench is characterized by very weak concentration fluctuations which can be only detected by atomic sensitive techniques. The atom probe, thanks to its spatial (1 nm) and mass resolution, is an appropriate technique to study the interconnected α–α' network developed on a nanometer scale during spinodal decomposition [12, 13]. From atom probe data, the extent of the spinodal amplitude in the ferrite phase can be quantified

0953-8984/99/041105+10$19.50

by the statistical distance (called variation V) between experimental and binomial chromium concentration frequency distribution [14]. The statistical distance is the difference between the area of the two distributions. Since these two distributions are normalized, V varies in the range of 0 (homogeneous) to 2 (completely decomposed). However, when V is smaller than about 0.05–0.1, the result has to be interpreted with care because of statistical fluctuations in the atom probe set of data [10].

Mössbauer spectrometry has already proved effective in studying ferrite decomposition [5, 6, 8, 15, 16]. Indeed, α' domains can be easily detected since it is weakly magnetic or non-magnetic as a function of chromium content, whereas α is strongly magnetic. But, for duplex steels, the study is complicated by the presence of the paramagnetic γ phase. In a previous paper [11], we described an original method for paramagnetic austenite extraction, which enables us to study the first stages of the ferrite transformation in duplex steels.

In this paper, we present Mössbauer studies on the quenching rate influence on ferrite decomposition in order to clarify the mechanism of the first stages of transformation. These results will be compared to the atom probe results to demonstrate the efficiency of the two techniques. Moreover, the hyperfine field distributions are studied to characterize the local environment of the ^{57}Fe in the decomposed ferrite.

2. Experiment

The samples were supplied by Electricité de France. The specimen composition and the corresponding ferrite composition are reported in table 1. The parallelepiped-shaped samples ($15 \times 11 \times 0.4$ mm) were machined from a cast which was solution treated for three hours at 1080 °C and then quenched. The cast is about 120 mm thick, so the local quenching rate (Q) of each sample depends on the depth at which it was taken. Q is estimated to be 2 °C s^{-1} in the core and 10 °C s^{-1} close to the surface. To expand the studied domain of quenching rates, a thin specimen was re-solution treated at 1080 °C s^{-1} and then water quenched. Q is then estimated to be 20 °C s^{-1}. Moreover, the properties of unaged specimens are compared with those of two thermally aged specimens (2500 h at 350 °C and 400 °C).

Table 1. Bulk composition of the specimen measured by electron microprobe, and ferrite composition measured by atom probe. The ferrite content of the specimen obtained with a sigma-meter, is about 30%.

Component	Cr	Ni	Mo	C	Si	Mn	Fe
Specimen (% atom)	22.0	8.9	1.4	0.14	2.0	0.9	64.5
Ferrite (% atom)	25.0	6.6	2.6	0	2.7	0.5	62.3

After mechanical polishing, samples were analysed by CEMS, which analyses the first 200 nm in depth from the sample surface. The spectra were recorded at room temperature using a conventional spectrometer equipped with a home-made helium-methane proportional counter. The source was ^{57}Co in a rhodium matrix. The Mössbauer spectra were fitted using a least-squares technique by the histogram method related to discrete distribution. The isomer shift (IS) at ^{57}Fe nuclei is given relative to α-Fe at room temperature. All the details concerning the atom probe analysis of the same specimens are given in a previous paper [10].

3. Microhardness, Mössbauer and atom probe results correlated with the quenching rate (Q)

Atom probe and microhardness measurements were carried out in the ferritic phase. All the results are summarized in table 2.

Table 2. Specimen characteristics, microhardness and atom probe results.

Specimen number	Quenching rate (°C s^{-1})	Treatment	Microhardness HV (0.05)	V
a	2	unaged	348 ± 21	0.15 ± 0.03
b	5	unaged	—	0.16 ± 0.05
c	5	unaged	—	0.14 ± 0.03
d	5	unaged	304 ± 25	0.08 ± 0.03
e	20	unaged	—	0.07 ± 0.02
f	2	2500 h–350 °C	600 ± 65	0.58 ± 0.06
g	2	2500 h–400 °C	740 ± 80	1.00 ± 0.07

For unaged specimens, whatever the quenching rate, microhardness is lower than for the aged samples f and g, in good agreement with the embrittlement of the steels during thermal ageing [2, 17]. But, microhardness of unaged specimens tends to increase with decreasing Q, in good agreement with the increase of the decomposition extent (given by V). Indeed, as Auger *et al* report [18], a linear relationship between V and $HV_{0.05}$ (Vickers microhardness) is observed in duplex steels. This behaviour is attributed to a hardening mechanism based on a α–α' misfit inducing an elastic stress. Thus, microhardness and V measurements show that the quenching rate is responsible for unaged specimen embrittlement. Nevertheless, both techniques are not accurate enough to study weakly decomposed states, because of the surrounding austenite, for hardness tests [18] and statistical fluctuations for V. This is the reason why the previous specimens were analysed by CEMS. The ^{57}Fe Mössbauer spectrum of duplex stainless steels consists of a central paramagnetic peak due to the austenite and a magnetic contribution due to the ferrite (figure 1). The mean isomer shift (IS) of the austenite is about -0.097 mm s^{-1}, which is in good agreement with the results of Solomon *et al* [8], and of the ferrite is about +0.01 mm s^{-1}, in good agreement with the measurements of Dubiel and Zubrowski [15]. The mean hyperfine field ($\langle B_{hf} \rangle$) of all specimens fluctuates around the mean value of 22 T (see table 3). The mean Mössbauer angle β, which corresponds to the mean angle between the atomic magnetic moments of iron and the normal to the plane of the surface of the sample, is close to 70° due to the mechanical polishing which tends to align moments in the sample plan. Despite a relatively good fit, it is impossible to show an upward or downward trend in the hyperfine parameters with Q because the austenite paramagnetic peak hides the low-field contribution due to the α' formation. The austenite is then extracted from the experimental spectrum in order to obtain only the experimental ferrite spectrum [11].

The ferrite spectra obtained in this way are represented in figure 2, as well as the corresponding hyperfine field distribution. The spectra consist of six broadened peaks similar to pure ferritic steel spectra [8]. The hyperfine distributions look like a Gaussian curve, but are somewhat broader and asymmetric. For a better understanding, the hyperfine field distributions of the two aged specimens are represented in figure 3(a), as well as the ferrite spectrum of the sample g (figure 3(b)). For the very decomposed specimen, g, the distribution has two contributions attributed to the α and α' domain. Indeed, in the α Fe-enriched domain, ^{57}Fe is mainly surrounded by Fe atoms, whereas in α' domains it is surrounded preferentially by Cr atoms. As chromium decreases the hyperfine field, the two domains α and α' give, respectively,

Table 3. Mean hyperfine field of the ferrite.

Specimen number	$\langle B_{hf} \rangle$ (T)$^{(1)}$ ($\pm$0.5 T)	$\langle B_{hf} \rangle$ (T)$^{(2)}$ ($\pm$0.1 T)
a	21.8	22.0
b	22.4	21.9
c	22.2	21.7
d	23.1	21.6
e	21.1	21.3
f	21.2	22.2
g	22.7	22.0

(1) Obtained by fitting the whole spectrum.
(2) Obtained after extracting the austenite contribution.

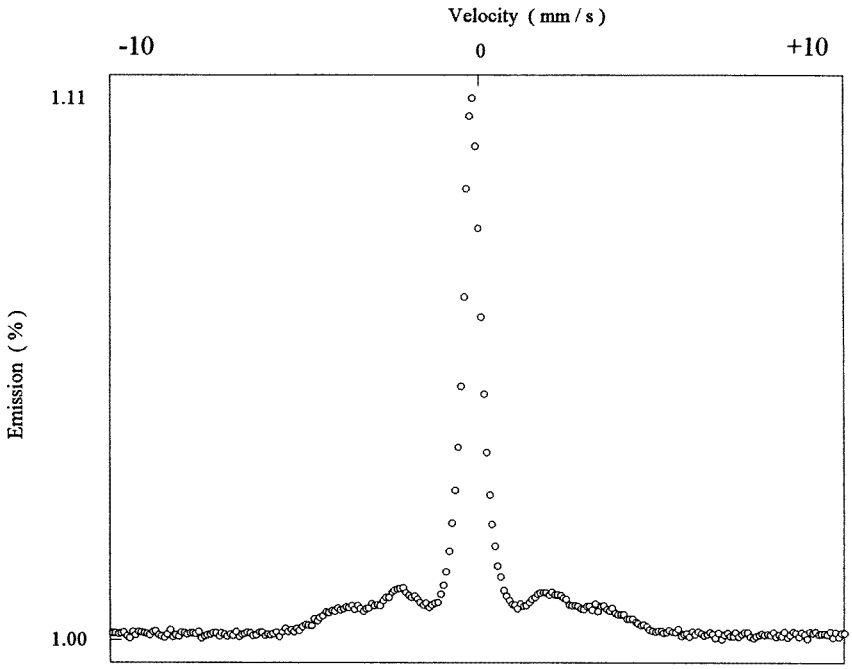

Figure 1. CEMS experimental spectrum of specimen e.

a high field and a low field contribution in the distribution. For the specimen with a lower ageing time, f, the concentration of α and α' domains are too close to separate one from the other in the hyperfine field distribution. Nevertheless, the distribution has a 'bump' at about 16 T which seems to reveal that two contributions overlap. For unaged specimens, the hyperfine field distributions do not show these two contributions. However, the mean hyperfine field of the distributions varies with the Q values. For $Q = 2$, 5 and 20 °C s^{-1}, $\langle B_{hf} \rangle = 22.0$, 21.7 and 21.3 T respectively, indicating a change in the ferrite of unaged specimens. This change can be interpreted as follows: the slower a specimen is quenched, the longer it remains under the miscibility gap and so the more decomposed it is. From the distribution shape it is impossible to know whether the transformation is nucleation and growth or of a spinodal type. The recent works of Cieslak and Dubiel [19] using Mössbauer effect modelling in an Fe–Cr

alloy, predict that the most pronounced difference between the two regimes of decomposition occurs at the middle stages of the decomposition. At the early stages, the difference is too weak to distinguish between the two. It is all the more difficult in our case because of the influence of the other elements (mainly Ni).

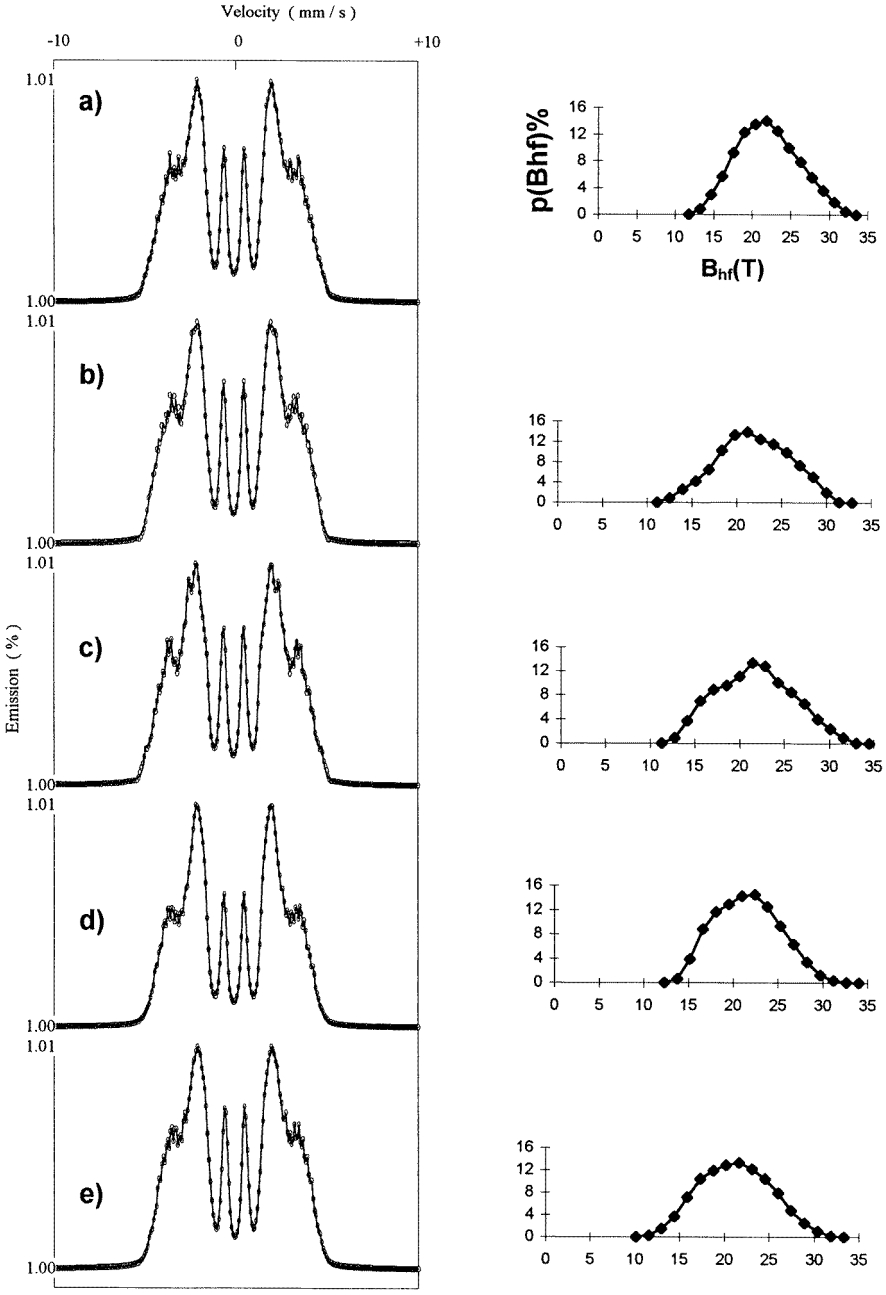

Figure 2. Ferrite experimental spectra of the specimens defined in table 2 and the corresponding hyperfine field distributions.

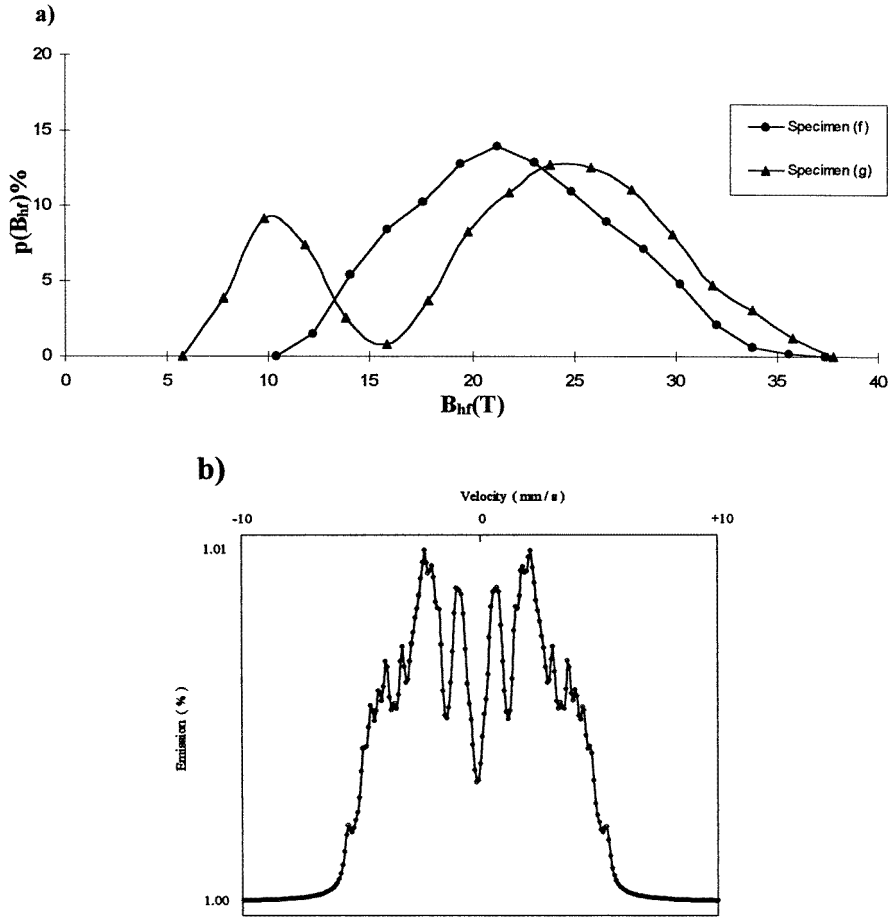

Figure 3. (a) Hyperfine field distributions of the ferrite of the f and g specimens. (b) Ferrite experimental spectrum of the g specimen.

4. Comparison of Mössbauer and atom probe results

Other specimens cut off in the depth of a cylindrical shaped material (figure 4(a)) were analysed by the two techniques.

$\langle B_{hf} \rangle$ is maximum (22 T) in the core and minimum at the surfaces (21.5 T) (see figure 4(b)). This is in good agreement with the previous results. Indeed, $\langle B_{hf} \rangle$ is maximum in the core where the Q is the smallest ($2\,^{\circ}\mathrm{C\ min}^{-1}$), thus where the decomposition is more pronounced. In addition, the $\langle B_{hf} \rangle$ profile is asymmetric, and $\langle B_{hf} \rangle$ is bigger at the internal surface than at the external. This can be explained by the fact that on the internal side the water gets warm because it is confined, so the thermal exchanges are slower and the transformation is more important.

The atom probe results are given figure 4(c). In order to compare CEMS and atom probe results, $\langle B_{hf} \rangle$ is plotted against V (figure 5(a)). $\langle B_{hf} \rangle$ increases linearly with V for the unaged specimen ($V < 0.2$). For the two aged specimens ($V = 1.00$ and $V = 0.58$), it is almost constant at about 22 T. This saturation is related to the moving of the two contributions

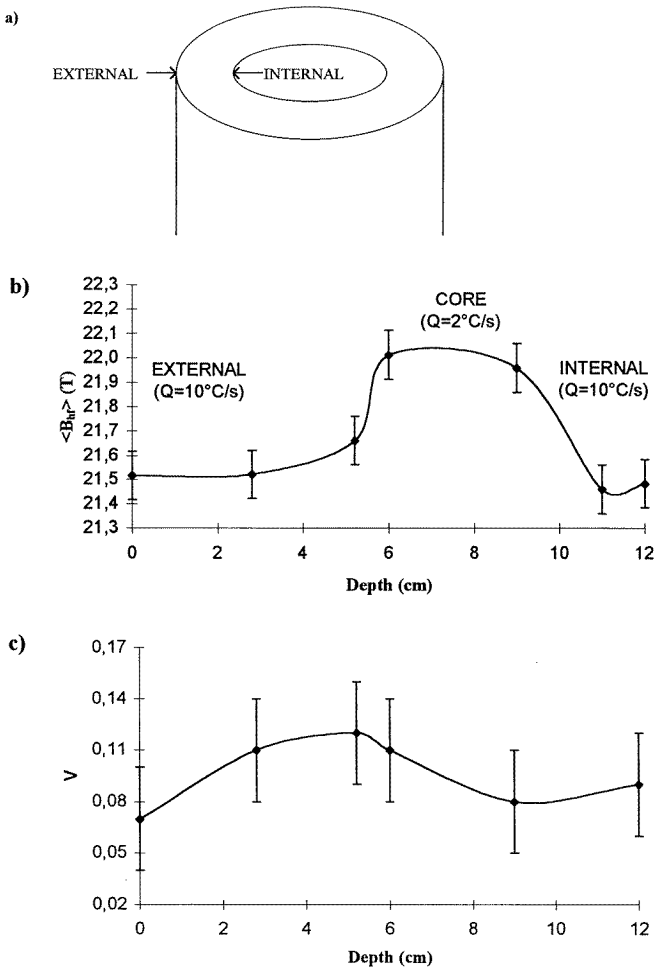

Figure 4. (a) Cylindrical material. (b) $\langle B_{hf} \rangle$ versus the depth. (c) V versus the depth.

corresponding to α and α', one towards high field (α) and the other towards low field (α'). This is seen by plotting the mean hyperfine field of the α domain only for the two aged specimens (figure 5(b)). Then, $\langle B_{hf} \rangle$ increases linearly whatever V. Moreover, for $V = 2$, the linear extrapolation gives $\langle B_{hf} \rangle = 28.9$ T, which is in good agreement with the results on the ageing effects on the ferritic phase [8]. However, values are very scattered for $V < 0.2$ because the atom probe parameter (V) is less accurate than $\langle B_{hf} \rangle$ during the first stages of the ferrite decomposition (see the error bars). This explains the difference between figures 4(b) and (c).

In conclusion, CEMS is well equipped to study the first stages of the ferrite transformation in duplex stainless steels.

5. Hyperfine field and local environment in the ferrite

As shown previously, the mean hyperfine field is a pertinent parameter to follow the first stages of ferrite transformation. But, the field distributions also give important information on the chemical order and concentration value in the ferritic phase. Indeed, when ferrite

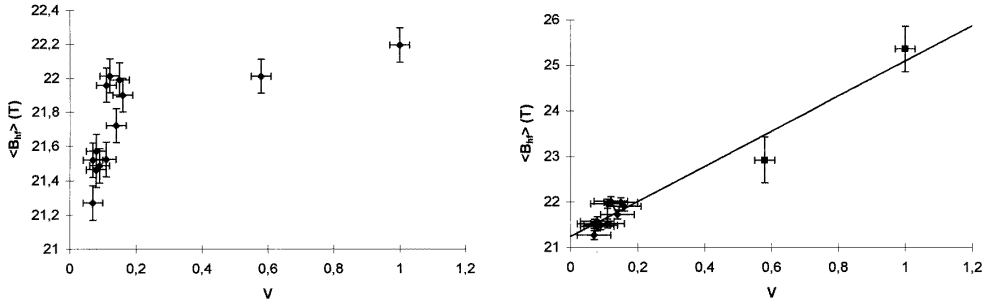

(a) (b)

Figure 5. (a) $\langle B_{hf}\rangle$ of the whole hyperfine field distributions versus V. (b) $\langle B_{hf}\rangle$ of the whole hyperfine field distribution for ($V < 0.2$) and of the α contribution for $V > 0.2$.

is not decomposed or is weakly decomposed, the B_{hf} distribution has a Gaussian profile, indicating random distribution of all the atoms. During the decomposition, the broadening of the distributions indicates a non-random distribution of the atoms. This is due to the formation of α and α' domains in which the nearest-neighbours of iron atoms are different.

In a ternary alloy (Fe, Cr, Ni), a simple model can be used to calculate the hyperfine field $B(m_1, m_2, n_1, n_2)$ corresponding to an ^{57}Fe environment

$$B(m_1, m_2, n_1, n_2) = B_0 - a_1 m_1 - a_2 m_2 - b(n_1 + n_2) \tag{1}$$

where m, n are the numbers of Cr and Ni atoms respectively, and the numbers 1 and 2 denote the nearest-neighbour and the next nearest-neighbour shell respectively. B_0, a_1, a_2, and b are iteration parameters. For the bcc ferrite structure, each atom has eight nearest-neighbours and six next nearest-neighbours. For a simplification, b is assumed to be common to n_1 and n_2 [23]. The probability of a Fe nuclei having a neighbouring configuration (m_1, m_2, n_1, n_2) is assumed to be given by a random distribution:

$$P(m_1, m_2, n_1, n_2) = C_8^{m_1} C_{8-m_1}^{n_1} C_6^{m_2} C_{6-m_2}^{n_2} X_{Fe}^{(14-m_1-m_2-n_1-n_2)} X_{Cr}^{(m_1+m_2)} X_{Ni}^{(n_1+n_2)} \tag{2}$$

where X_{Fe}, X_{cr} and X_{Ni} are the iron, chromium and nickel concentrations respectively.

A calculated distribution is obtained considering that the relative intensities are proportional to the probabilities. The calculation was performed considering that the configurations with $P < 1.5\%$ can be neglected.

The hyperfine field distribution of the specimen e was calculated using the random distribution (figure 6(a)). The best fit of the calculated distribution with the experimental one gives the concentrations: Fe, 72 at.%, Cr, 22 at.% and Ni, 6 at.%. These data are in good agreement with the atom probe results. The differences between calculated and experimental distributions tend to prove that Fe, Cr and Ni atoms are not completely randomly distributed, thus, despite a very fast quench ($Q = 20\,^{\circ}\mathrm{C\ s^{-1}}$) the ferrite is somewhat decomposed. Nevertheless, the approximations used in the model might also cause differences between calculated and experimental results. Moreover, figure 6(b) shows that B_{hf} at the iron nucleus decreases linearly as the number of Cr neighbour Fe atoms increases. This is in good agreement with previous results in stainless steels [20]. Changing an Fe atom to a Cr atom in nearest-neighbour decreases B_{hf} at about $a_1 = 2.4$ T, which is slightly smaller than the 3.2 T for Fe–Cr alloys [15]. The smaller decrease can be attributed to the magnetic atoms Ni. The empirical relation giving the concentration dependence of the mean hyperfine field in the ferrite of a duplex stainless steel is then $\langle B_{hf}\rangle = 29.5 - 0.27X$, X being the chromium content (%).

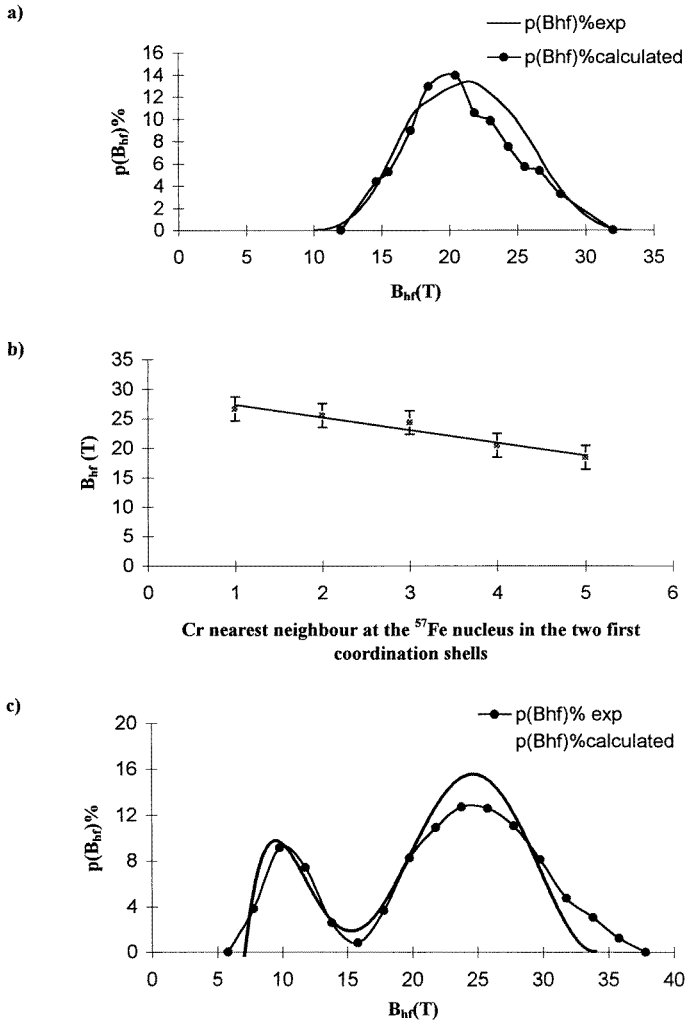

Figure 6. (a) Calculated and experimental field distributions of the specimen e ($Q = 20\,^{\circ}\mathrm{C\ s^{-1}}$). (b) B_{hf} versus the Cr nearest neighbour at the ^{57}Fe nucleus in the first two coordination shells. (c) Calculated and experimental field distributions of the specimen g aged for 2500 h at 400 °C.

The hyperfine field distribution of the specimen g was also calculated, assuming that the two contributions are two random distributions (figure 6(c)). The α and α' domain chromium concentrations giving the best fit are 25 at.% and 70 at.% respectively. In the α' domains, a ^{57}Fe atom is more likely to be surrounded by 5, 6 or 7 chromium atoms in the first co-ordination shell, whereas in the α domain it has 1, 2 or 3 chromium as neighbours. The differences between calculated and experimental distributions about high fields (>33 T) are due to the influence of Ni atoms. The latter segregates into Fe enriched domains and increases B_{hf}. This segregation in duplex stainless steels was previously observed [21, 22]. There is also an overlap between α and α' calculated distributions about 15 T, which might deteriorate all the results. From the empirical relation obtained previously, the α and α' chromium concentrations are 17 at.% and 72 at.% respectively. These results are in good agreement with those obtained

from the fit. Moreover, at a rough estimate, the α'/α ratio is $1/4$. It is difficult to determine those proportions with the phase diagram rule on the Fe–Cr equilibrium diagram since the miscibility gap is very modified due to the presence of other atoms such as Ni and Mo. In particular, Ni is known to promote spinodal decomposition [7, 8]. In addition, the use of two random distributions for α and α' seems to give results in agreement with previous results, hence, even if not demonstrated, the random character of the α and α' cannot be rejected.

6. Conclusion

This work demonstrates that the quenching rate is responsible for ferrite embrittlement of unaged duplex stainless steels. This embrittlement cannot be attributed to a nucleation and growth process or a spinodal type decomposition because it concerns the early stages of the decomposition.

All the results also prove that Mössbauer spectrometry is appropriate to studying the very weak transformation. The $\langle B_{hf} \rangle$ of the hyperfine field distributions enables us to determine the decomposition state of ferrite of a duplex stainless steel, even for the early stages of the transformation. Moreover, from the hyperfine field distributions, the chromium concentration is about 25% and 70% in the α and α' domains respectively and the ratio α'/α is $1/4$. These results are difficult to obtain by other techniques.

Acknowledgment

This research is financially supported by Electricité de France, Département Etude des Matériaux, under contract EDF/CNRS No 509511.

References

[1] Bonnet S, Bourgoin J, Champredonde J, Guttmann D and Guttmann M 1990 *Mater. Sci. Technol.* **6** 221
[2] Miller M K, Bentley J, Brenner S S and Spitznagel J A 1984 *J. Physique* C **45** 385
[3] Sassen J M, Hetherington M G, Godfrey T J and Smith G D W 1987 *Proc. of Int. Conf. on Properties of Stainless Steels in Elevated Temperature Service (ASME Winter Annual Meeting) (Boston, 13–18 Dec. 1987)* ed M Prager (New York) pp 65–78
[4] LaSalle J C and Schwartz L H 1986 *Acta Metall.* **34** 989
[5] Chandra D and Schartz L H 1971 *Metall. Trans.* **2** 511
[6] De Nys and Gierler P M 1971 *Metall. Trans.* **2** 1423
[7] Ishikawa Y, Yoshimura T, Mokiai A and Kuwano H 1995 *Met. Trans.* **2** 1423
[8] Solomon H D and Levinson L M 1978 *Acta Metall.* **26** 429
[9] H Pollak, Karfunkel U, Lodya J A and Mala N 1994 *Hyp. Int.* **94** 2355
[10] Hedin M, Massoud J P and Danoix F 1996 *J. Physique* C **6** 235
[11] Lemoine C, Fnidiki A, Teillet J, Hédin M and Danoix F 1998 *Scripta Mater.* **39** 61
[12] Godfrey T J and Smith G D W 1986 *J. Physique* C **47** 217
[13] Miller M K, Hyde J M *et al* 1995 *Acta Metall.* **43** 3385
[14] Blavette D, Grancher G and Bostel A 1988 *J Physique* C **49** 433
[15] Dubiel S M and Zubrowski J 1981 *J. Magn. Magn. Mater.* **23** 214
[16] Kuwano H 1985 *Trans. Japan Inst. Met.* **26** 473
[17] Brenner S S, Miller M K and Soffa K A 1982 *Scripta Met.* **16** 831
[18] Auger P, Danoix F *et al* 1995 *Ann. Phys., Paris* C **20** 3–143
[19] Cieslak J and Dubiel S M 1998 *J. Alloys Compounds* **269** 208
[20] Fa-Shen Li, Ji-Jun Sun and Chien C L 1995 *J. Phys.: Condens. Matter* **7** 1921
[21] Yoshimura T and Ishikawa Y 1992 *J. Japan. Inst. Met.* **56** 873
[22] Danoix F, Deconihout B, Bostel A and Auger P 1992 *Surf. Sci.* **266** 409
[23] Vincze L and Campbell I A 1973 *J. Phys. F: Met. Phys.* **3** 647